Dynamics of Shell-and-Tube Heat Exchangers to Arbitrary Temperature and Step Flow Variations

Y. Xuan and W. Roetzel
Inst. of Thermodynamics, University of the Federal Armed Forces Hamburg, D-2000 Hamburg 70, Germany

A versatile and efficient method is developed for predicting dynamic performances of parallel and counterflow heat exchangers subject to arbitrary temperature variations and step flow disturbances, including the effect of flow maldistribution and the influence of heat capacities of both fluids, shell wall and tube bank as well as nonzero initial temperatures. Two algorithms of numerical inversion of the Laplace transform are introduced to determine the final temperature profiles in the real-time domain and some examples are calculated with nonuniform initial conditions. The accuracy of the proposed method is demonstrated with the calculated results at new steady states. Experiments are carried out on a labor-sized heat exchanger to further examine the feasibility of this method and the comparison between calculated and measured temperature profiles is illustrated and discussed.

Introduction

As parts of a system, heat exchangers are widely used in many industrial processes and frequently undergo transient performances which may result from the external load regulations or accidents. In these cases, temperatures and flow rates of fluids into heat exchangers will be changed. Generally, the analysis of transient responses of heat exchangers is separated into two aspects: the response to temperature transients and the response to flow transients. Extensive research articles (Romie, 1984, 1985; Correa and Marchetti, 1987; Roetzel and Xuan, 1992a) have been devoted to the first. However, they neglected the effect of heat capacities of tube wall and shell on transient behavior and presumed the uniform initial temperature distribution. On the contrary, less attention has been focused on the latter. Yang (1964) used a linearized model to study the response to flow rate disturbance and gave the one-order perturbation solution for step, linear, and exponential transients. Tan and Spinner (1978) derived the exact solution to the response to a step change in the fluid velocity. However, both articles made the assumption of uniform shellside fluid temperature and considered only the temperature response of tubeside fluid. Ratel et al. (1992) applied the finite-difference method to describing transient performance of shell-and-tube heat exchangers, in which they divided a whole apparatus into several sections and solved transient equations by using a time step. This method may cost much computation time, especially when one wants to determine the thermal performance corresponding to a long span of time or the new steady state. By means of rectangular grids of real-time and space coordinates, Tan and Spinner (1984) applied the characteristics method to continuous countercurrent processes in the nonsteady state.

All the previously mentioned articles are based on the conventional plug-flow model which is so far considered to be the standard model for both steady-state and transient simulations of shell-and-tube heat exchangers. It assumes that the flow is identical everywhere and there occur no flow maldistributions—bypass, leakage streams, and backmixing, for example. Such maldistributions will degrade thermal performance of heat exchangers. The actual flow, especially the shellside flow, is very complicated and various forms of flow maldistribution may exist (Tinker, 1951). In these cases, the ideal plug-flow greatly deviates from the real flow pattern. One implement to correct this deviation is the dispersion model which is based on a dispersed plug flow, that is, the main plug flow with longitudinal dispersion or mixing. It has been mainly applied to flow in empty tubes and packed beds. To the best of our knowledge, so far no articles on application of the dispersion model to dynamic simulation have been published by others.

Furthermore, the initial uniform temperature distributions have been widely assumed to facilitate the mathematical deduction, although this often violates the actual situation. Heat capacities of solid components such as tube wall, baffles, and shell exert some influence on transient responses of exchangers

Correspondence concerning this article should be addressed to W. Roetzel.
Y. Xuan is currently at Dept. 8, East China Institute of Technology, Nanjing, P.R. China.

and should not be eliminated. In spite of the fact that both temperature and flow transients may simultaneously occur and affect the performance of heat exchangers, until now the influences of temperature and flow rate changes have been isolated from each other in the analysis for the convenience of mathematical treatment.

In the previous works (Roetzel and Xuan, 1992a,b), the dispersion model has been used to tackle transient responses to only temperature variations under uniform or specially designated nonzero initial conditions. This article attempts to derive a versatile and efficient method for predicting transient behavior of heat exchangers, including as many influence factors as possible. The method is based upon the dispersion model rather than the conventional plug-flow model to deal with the possible shellside maldistribution. Heat capacities of both shell and tubeside fluids, tube bundle and shell are included in the governing equations. This method is extended to such cases that arbitrary temperature changes and step flow disturbance simultaneously exert influence on the transient heat-transfer process. The general form of nonzero initial temperature profiles as well as parallel and counterflow arrangements is involved. The numerical inversion of the Laplace transform is applied to determine the final solution. The experiment is carried out on a labor-sized heat exchanger with baffles to estimate the feasibility of the theoretical method.

Governing Equations

Since the longitudinal heat conduction in the tube wall is generally negligible, no term for this influence is inserted in the governing equations. Constant thermal properties of both fluids and solid materials are assumed. The other presumptions include the infinite heat conductivity of tube wall perpendicular to the flow direction and zero heat flux transferred from the apparatus to the environment. As done in the previous work (Roetzel and Xuan, 1992), the effect of flow maldistribution on thermal performance is modeled by introducing an apparent heat conduction term in the energy balance, which is the essence of the dispersion model. Therefore, the dispersion model takes the form of a parabolic partial differential equation. In the following analysis, the tubeside flow is considered as plug flow and the shellside maldistribution is involved because of the shellside complicated configuration which may induce nonuniform distribution of flow such as bypassing, leakage stream, and backmixing. If necessary, the dispersion model could be simultaneously used for the tubeside process without any additional difficulty.

Figure 1 schematically shows an exchanger with parallel or counterflow arrangement. The residence times τ_{r1} and τ_{r2} of both fluids and the following dimensionless variables as well as other parameters are introduced as follows:

$$\tau_{r1}=\frac{C_1}{\dot{W}_1},\quad \tau_{r2}=\frac{C_2}{\dot{W}_2},\quad z=\frac{\tau}{\tau_{r1}},\quad x=\frac{\ell}{L},\quad R_\tau=\frac{\tau_r^2}{\tau_{r1}},\quad R_1=\frac{\dot{W}_1}{\dot{W}_2}=\frac{1}{R_2}$$

$$R_{c1}=\frac{C_1}{C_2}=\frac{R_1}{R_\tau}=\frac{1}{R_{c2}},\quad R_w=\frac{C_w}{C_1+C_2},\quad R_s=\frac{C_s}{C_w},\quad U_s=\frac{(hA)_s}{\dot{W}_1}$$

$$U_1=\frac{(hA)_1}{\dot{W}_1},\quad U_2=\frac{(hA)_2}{\dot{W}_2},\quad \alpha_1=\frac{U_1}{1+R_{c2}},\quad \alpha_2=\frac{U_2}{R_\tau(1+R_{c1})}$$

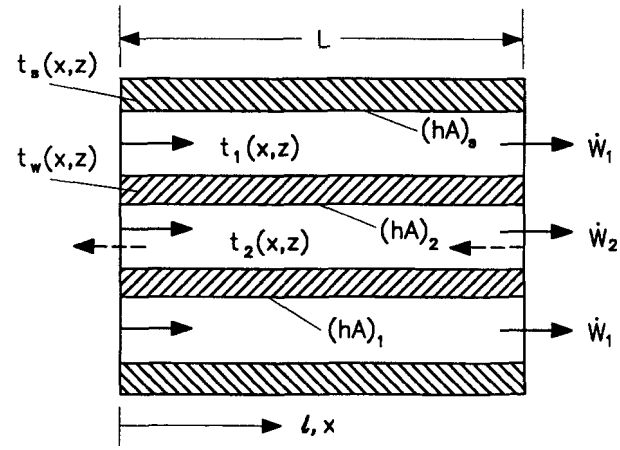

Figure 1. Schematic representation of parallel and counterflow heat exchangers.

where C_w may include heat capacity of baffles. One can obtain governing differential equations by the principle of energy balance to confine the transient behavior:

$$\frac{1}{Pe}\frac{\partial^2 t_1}{\partial x^2}-\frac{\partial t_1}{\partial x}-\frac{\partial t_1}{\partial z}-U_1(t_1-t_w)-U_s(t_1-t_s)=0 \tag{1}$$

$$\text{sign}\frac{\partial t_2}{\partial x}+R_\tau\frac{\partial t_2}{\partial z}+U_2(t_2-t_w)=0 \tag{2}$$

$$R_w\frac{\partial t_w}{\partial z}-\alpha_1(t_1-t_w)-\alpha_2(t_2-t_w)=0 \tag{3}$$

$$R_sR_w(1+R_{c2})\frac{\partial t_s}{\partial z}-U_s(t_1-t_s)=0 \tag{4}$$

where the positive sign (+) and the negative (−) of sign (±) in Eq. 2 are pertinent to parallel and counterflow, respectively. The Péclet number Pe appearing in Eq. 1 is defined as $Pe=(\dot{W}_1L)/(\mathfrak{D}A_q)$ and takes the effect of the shellside maldistribution on thermal process into account. Its value depends upon the intensity of axial mixing and maldistribution. The stronger the maldistribution, the smaller the Péclet number and the poorer the thermal performance. $Pe\to 0$ means complete axial mixing; if $Pe\to\infty$, the dispersion model approaches the conventional plug-flow model. The actual flow pattern in heat exchangers confines values of Pe in the range $0<Pe<\infty$. The boundary condition for the shellside flow should take the Dankwerts' form of the sake of energy conservation to correspond to the dispersion model (Xuan, 1991)

$$t_1-\frac{1}{Pe}\frac{\partial t_1}{\partial x}=f_1(z)\ \text{ at }\ x=0\ \text{ and }\ \frac{\partial t_1}{\partial x}=0\ \text{ at }\ x=1 \tag{5}$$

For the tubeside flow one has

$$t_2(0,z)=f_2(z)\ \text{ for parallel flow}$$
$$\text{or }\ t_2(1,z)=f_2(z)\ \text{ for counterflow} \tag{6}$$

The general forms of initial temperature profiles can be represented as:

$$t_1(x,0)=g_1(x),\quad t_2(x,0)=g_2(x),\quad t_w=(x,0)=g_w(x)$$
$$\text{and}\quad t_s(x,0)=g_s(x) \qquad (7)$$

Using the subscript 'r' to express the initial state before step change of the flow velocity (from u_r to u) and defining $\sigma_1 = u_1/u_{1r}$ and $\sigma_2 = u_2/u_{2r}$, one can rewrite the thermal flow rates $\dot{W}_1$, $\dot{W}_2$ and the aforedefined dimensionless parameters as follows:

$$\dot{W}_1=\sigma_1\dot{W}_{1r},\quad \dot{W}_2=\sigma_2\dot{W}_{2r},\quad \tau_{r1}=\frac{\tau_{r1r}}{\sigma_1},$$
$$\tau_{r2}=\frac{\tau_{r2r}}{\sigma_2},\quad R_1=\frac{\sigma_1}{\sigma_2}R_{1r},\quad R_\tau=\frac{\sigma_1}{\sigma_2}R_{\tau r}$$

If the flow pattern remains the same, that is, the laminar or turbulent flow before and after step flow change, the heat-transfer coefficients h_1 and h_2 could be expressed as

$$h_1=\sigma_1^{n_1}h_{1r}\quad\text{and}\quad h_2=\sigma_2^{n_2}h_{2r} \qquad (8)$$

where the exponent n_1 depends upon the value of the Reynolds number, the geometric characteristics, and the arrangement of a tube bank. The average value for in-line bank is $n_1=0.63$ and for staggered bank $n_1=0.6$ in the range $10^3<Re_1<2\times10^5$ (Zukauskas and Ulinskas, 1988). The exponent n_2 depends upon the flow pattern in tubes and $n_2=0.8$ for the fully developed turbulent flow in a smooth circular tube (Incropera and DeWitt, 1985). Therefore, the new forms of the other parameters follow

$$U_1=\sigma_1^{n_1-1}U_{1r},\quad U_2=\sigma_2^{n_2-1}U_{2r},\quad \alpha_1=\alpha_{1r}\sigma_1^{n_1-1},\quad \alpha_2=\alpha_{2r}\frac{\sigma_2^{n_2}}{\sigma_1}$$

According to the given initial conditions, application of the Laplace transform to Eqs. 1-4 yields the different forms of these equations in the image domain by using the Laplace parameter s with respect to the dimensionless time variable z

$$\frac{d^2T_1}{dx^2}-Pe\frac{dT_1}{dx}-b_{11}T_1-b_{12}T_2=-G_1(x) \qquad (9)$$

$$\frac{dT_2}{dx}-b_{21}T_1-b_{22}T_2=G_2(x) \qquad (10)$$

$$T_w=\frac{\alpha_1T_1+\alpha_2T_2}{\alpha_1+\alpha_2+R_ws}+\frac{R_wg_w(x)}{\alpha_1+\alpha_2+R_ws} \qquad (11)$$

$$T_s=\frac{U_sT_1}{U_s+R_sR_w(1+R_{c2})s}+\frac{R_sR_w(1+R_{c2})g_s(x)}{U_s+R_sR_w(1+R_{c2})s} \qquad (12)$$

where

$$b_{11}=\left[s+U_1+U_s-\frac{\alpha_1U_1}{\alpha_1+\alpha_2+R_ws}-\frac{U_s^2}{U_s+R_sR_w(1+R_{c2})s}\right]Pe$$

$$b_{12}=-\frac{\alpha_2U_1Pe}{\alpha_1+\alpha_2+R_ws},\quad b_{21}=\frac{\text{sign}\,\alpha_1U_2}{\alpha_1+\alpha_2+R_ws},$$

$$b_{22}=\text{sign}\left(\frac{\alpha_2U_2}{\alpha_1+\alpha_2+R_ws}-R_\tau s-U_2\right)$$

$$G_1(x)=Pe\left[g_1(x)+\frac{U_1R_wg_w(x)}{\alpha_1+\alpha_2+R_ws}+\frac{U_sR_sR_w(1+R_{c2})}{U_s+R_sR_w(1+R_{c2})s}g_s(x)\right]$$

$$G_2(x)=\text{sign}\left[R_\tau g_2(x)+\frac{U_2R_wg_w(x)}{\alpha_1+\alpha_2+R_ws}\right]$$

Introducing the mathematical operator D for "d/dx," one can obtain:

$$[D^3-(Pe+b_{22})D^2+(Peb_{22}-b_{11})D+b_{11}b_{22}-b_{12}b_{21}]T_1$$
$$=b_{12}G_2(x)-(D-b_{22})G_1(x) \qquad (13)$$

It is easy to derive a general solution to the homogeneous differential equation corresponding to the nonhomogeneous differential Eq. 13

$$T_1^*=A_1\exp(\beta_1x)+A_2\exp(\beta_2x)+A_3\exp(\beta_3x) \qquad (14)$$

where β_i ($i=1$, 2, and 3) are three roots of the following equation:

$$\beta^3-(Pe+b_{22})\beta^2+(Peb_{22}-b_{11})\beta+b_{11}b_{22}-b_{12}b_{21}=0 \qquad (15)$$

The nonhomogeneous part of Eq. 13 should be known in advance. This part depends upon the instant that inlet temperature variations and flow disturbance occur. It is a common case that these inlet changes begin after the previous steady state has been reached. Without loss of generality, the solution to Eq. 13 is derived with such initial temperature distributions in the following analysis.

Initial Temperature Distributions

In the light of the aforedescribed procedure of setting up Eqs. 1-4, one can determine the initial temperature profiles corresponding to the previous steady state

$$g_1(x)=a_1\exp(\lambda_1x)+b_1\exp(\lambda_2x)+\epsilon_3 \qquad (16)$$

$$g_2(x)=a_2\exp(\lambda_1x)+b_2\exp(\lambda_2x)+\epsilon_3 \qquad (17)$$

$$g_w(x)=m_1\exp(\lambda_1x)+m_2\exp(\lambda_2x)+\epsilon_3 \qquad (18)$$

$$g_s(x)=g_1(x) \qquad (19)$$

where

$$a_1=\frac{\epsilon_1}{\lambda_1},\quad b_1=\frac{\epsilon_2}{\lambda_2},\quad a_2=\frac{\chi_1\epsilon_1}{\lambda_1(\chi_1+\lambda_1)},\quad b_2=\frac{\chi_1\epsilon_2}{\lambda_2(\chi_1+\lambda_2)}$$

$$m_1=\frac{a_1R_{1r}U_{1r}+a_2U_{2r}}{R_{1r}U_{1r}+U_{2r}},\quad m_2=\frac{b_1R_{1r}U_{1r}+b_2U_{2r}}{R_{1r}U_{1r}+U_{2r}}$$

$$\epsilon_1 = \frac{1}{\frac{1}{\lambda_1} - \frac{1}{Pe_r} - \frac{\chi_1 w_4}{\lambda_1(\chi_1+\lambda_1)} - \exp(\lambda_1-\lambda_2)\left[\frac{1}{\lambda_2} - \frac{1}{Pe_r} - \frac{\chi_1 w_5}{\lambda_2(\chi_1+\lambda_2)}\right]}$$

$$\epsilon_2 = -\exp(\lambda_1-\lambda_2)\epsilon_1,$$

$$\epsilon_3 = -\left[\frac{\chi_1 w_4}{\lambda_1(\chi_1+\lambda_1)} - \exp(\lambda_1-\lambda_2)\frac{\chi_1 w_5}{\lambda_2(\chi_1+\lambda_2)}\right]\epsilon_1$$

$$\lambda_{1,2} = \frac{(Pe_r-\chi_1) \pm \sqrt{(\chi_1-Pe_r)^2+4(\chi_1 Pe_r+\chi_2)}}{2}$$

$$\chi_1 = \text{sign}\frac{R_{1r}U_{1r}U_{2r}}{R_{1r}U_{1r}+U_{2r}}, \quad \chi_2 = \frac{U_{1r}U_{2r}}{R_{1r}U_{1r}+U_{2r}}Pe_r$$

$w_4 = 1$ and $w_5 = 1$ for parallel flow or $w_4 = \exp(\lambda_1)$ and $w_5 = \exp(\lambda_2)$ for counterflow. Thus, functions $G_1(x)$ and $G_2(x)$ in Eqs. 9 and 10 are respectively expressed by:

$$G_1(x) = \gamma_1 \exp(\lambda_1 x) + \gamma_2 \exp(\lambda_2 x) + \gamma_3 \tag{20}$$

$$G_2(x) = \rho_1 \exp(\lambda_1 x) + \rho_2 \exp(\lambda_2 x) + \rho_3 \tag{21}$$

where

$$\gamma_1 = Pe\left[a_1 + \frac{U_s R_s R_w(1+R_{c2})}{U_s+R_s R_w(1+R_{c2})s}a_1 + \frac{U_1 R_w}{\alpha_1+\alpha_2+R_w s}m_1\right]$$

$$\gamma_2 = Pe\left[b_1 + \frac{U_s R_s R_w(1+R_{c2})}{U_s+R_s R_w(1+R_{c2})s}b_1 + \frac{U_1 R_w}{\alpha_1+\alpha_2+R_w s}m_2\right]$$

$$\gamma_3 = Pe\,\epsilon_3\left[1 + \frac{U_s R_s R_w(1+R_{c2})}{U_s+R_s R_w(1+R_{c2})s} + \frac{U_1 R_w}{\alpha_1+\alpha_2+R_w s}\right]$$

$$\rho_1 = \text{sign}\left(R_r a_2 + \frac{U_2 R_w}{\alpha_1+\alpha_2+R_w s}m_1\right),$$

$$\rho_2 = \text{sign}\left(R_r b_2 + \frac{U_2 R_w}{\alpha_1+\alpha_2+R_w s}m_2\right)$$

$$\rho_3 = \text{sign}\,\epsilon_3\left(R_r + \frac{U_2 R_w}{\alpha_1+\alpha_2+R_w s}\right)$$

Transient Responses

Once the initial temperature profiles are derived, one is able to find the solution to the nonhomogeneous differential Eqs. 9 and 10. Two cases—the transient response to arbitrary inlet temperature variations and the response to both arbitrary temperature changes and step flow disturbance—might be possible. In the first case, it is easy to determine the final solution by means of the principle of superposition (Roetzel and Xuan, 1992b). In the second case, however, this superposition method fails since the inlet temperatures and flow disturbance simultaneously occur, and the steady and transient temperature profiles cannot be described by the same system of differential equations. To derive the solution to the above-mentioned nonhomogeneous equations subject to all these disturbances, the method of variation of parameters (Boyce and DiPrima, 1977) has been applied to Eqs. 9-10. According to the given boundary conditions and the aforederived general solution to the corresponding homogeneous equation, the transformed temperature profiles are obtained

$$T_1(x,s) = A_1\exp(\beta_1 x) + A_2\exp(\beta_2 x) + A_3\exp(\beta_3 x) + \frac{D_1}{A_0}\exp(\lambda_1 x) + \frac{D_2}{A_0}\exp(\lambda_2 x) - \frac{D_3}{A_0} \tag{22}$$

$$T_2(x,s) = A_1 e_1\exp(\beta_1 x) + A_2 e_2\exp(\beta_2 x) + A_3 e_3\exp(\beta_3 x) + e_4\exp(\lambda_1 x) + e_5\exp(\lambda_2 x) + e_6 \tag{23}$$

where

$$A_0 = \beta_2\beta_3(\beta_3-\beta_2) - \beta_1\beta_3(\beta_3-\beta_1) + \beta_1\beta_2(\beta_2-\beta_1)$$

$$A_1 = \frac{1}{\Delta}\Bigg\{E_1(s)[e_3 w_3\beta_2\exp(\beta_2) - e_2 w_2\beta_3\exp(\beta_3)] - \left(1-\frac{\beta_2}{Pe}\right)[e_3 Hw_3 - E_2(s)\beta_3\exp(\beta_3)] + \left(1-\frac{\beta_3}{Pe}\right)[e_2 Hw_2 - E_2(s)\beta_2\exp(\beta_2)]\Bigg\}$$

$$A_2 = \frac{1}{\Delta}\Bigg\{\left(1-\frac{\beta_1}{Pe}\right)[e_3 Hw_3 - E_2(s)\beta_3\exp(\beta_3)] - E_1(s)[e_3 w_3\beta_1\exp(\beta_1) - e_1 w_1\beta_3\exp(\beta_3)] + \left(1-\frac{\beta_3}{Pe}\right)[E_2(s)\beta_1\exp(\beta_1) - e_1 Hw_1]\Bigg\}$$

$$A_3 = \frac{1}{\Delta}\Bigg\{\left(1-\frac{\beta_1}{Pe}\right)[E_2(s)\beta_2\exp(\beta_2) - e_2 Hw_2] - \left(1-\frac{\beta_2}{Pe}\right)[E_2(s)\beta_1\exp(\beta_1) - e_1 Hw_1] + E_1(s)[e_2 w_2\beta_1\exp(\beta_1) - e_1 w_1\beta_2\exp(\beta_2)]\Bigg\}$$

$$\Delta = \left(1-\frac{\beta_1}{Pe}\right)[e_3 w_3\beta_2\exp(\beta_2) - e_2 w_2\beta_3\exp(\beta_3)] - \left(1-\frac{\beta_2}{Pe}\right)[e_3 w_3\beta_1\exp(\beta_1) - e_1 w_1\beta_3\exp(\beta_3)] + \left(1-\frac{\beta_3}{Pe}\right)[e_2 w_2\beta_1\exp(\beta_1) - e_1 w_1\beta_2\exp(\beta_2)]$$

$$D_1 = \left(\frac{\beta_3-\beta_2}{\lambda_1-\beta_1} + \frac{\beta_1-\beta_3}{\lambda_1-\beta_2} + \frac{\beta_2-\beta_1}{\lambda_1-\beta_3}\right)(b_{22}\gamma_1 - \gamma_1\lambda_1 + b_{12}\rho_1)$$

$$D_2 = \left(\frac{\beta_3-\beta_2}{\lambda_2-\beta_1} + \frac{\beta_1-\beta_3}{\lambda_2-\beta_2} + \frac{\beta_2-\beta_1}{\lambda_2-\beta_3}\right)(b_{22}\gamma_2 - \gamma_2\lambda_2 + b_{12}\rho_2)$$

$$D_3 = \left(\frac{\beta_3-\beta_2}{\beta_1} + \frac{\beta_1-\beta_3}{\beta_2} + \frac{\beta_2-\beta_1}{\beta_3}\right)(b_{22}\gamma_3 + b_{12}\rho_3)$$

$$e_1=\frac{\beta_1^2-Pe\beta_1-b_{11}}{b_{12}},\quad e_2=\frac{\beta_2^2-Pe\beta_2-b_{11}}{b_{12}},\quad e_3=\frac{\beta_3^2-Pe\beta_3-b_{11}}{b_{12}}$$

$$e_4=\frac{D_1(\lambda_1^2-Pe\lambda_1-b_{11})}{A_0b_{12}}+\frac{\gamma_1}{b_{12}},\quad e_5=\frac{D_2(\lambda_2^2-Pe\lambda_2-b_{11})}{A_0b_{12}}+\frac{\gamma_2}{b_{12}},$$

$$e_6=\frac{b_{11}D_3}{A_0b_{12}}+\frac{\gamma_3}{b_{12}}$$

$$E_1(s)=F_1(s)+\frac{D_1}{A_0}\left(\frac{\lambda_1}{Pe}-1\right)+\frac{D_2}{A_0}\left(\frac{\lambda_2}{Pe}-1\right)+\frac{D_3}{A_0}$$

$$E_2(s)=F_2(s)-e_4w_4-e_5w_5-e_6$$

$$H=-\frac{D_1\lambda_1}{A_0}\exp(\lambda_1)-\frac{D_2\lambda_2}{A_0}\exp(\lambda_2)$$

$w_1=1$ $\qquad w_1=\exp(\beta_1)$

$w_2=1$ for parallel flow or $w_2=\exp(\beta_2)$ for counterflow

$w_3=1$ $\qquad w_3=\exp(\beta_3)$

Thus, the transformed temperature profiles in the image domain have been determined according to the nonzero initial conditions in Eqs. 16-19. If the initial conditions take other forms, one can easily find the corresponding solution by using a similar procedure. Obviously, it is almost impossible to analytically perform inversion of the transformed solutions in Eqs. 22, 23, 11 and 12. The numerical inversion of the Laplace transform is used to finally obtain the transient behavior of heat exchangers. The calculation experience recommends two adaptable algorithms of the inversion—the numerical technique called Gaver-Stehfest algorithm (Stehfest, 1970) and the numerical inversion based on the Fourier series (Satoshi and Kiswhima, 1972). If the Laplace transform of the function $\mathfrak{f}(z)$ is defined by

$$\mathfrak{F}(s)=\int_0^\infty \mathfrak{f}(z)e^{-sz}dz,$$

the former is expressed by:

$$\mathfrak{f}(z)\cong\frac{\ln 2}{z}\sum_{i=1}^{M}K_i\mathfrak{F}\left(\frac{\ln 2}{z}i\right) \tag{24}$$

$$K_i=(-1)^{i+M/2}\sum_{k=(i+1)/2}^{\min(i,M/2)}\frac{k^{M/2}(2k)!}{(M/2-k)!\,k!\,(k-1)!\,(i-k)!\,(2k-i)!}$$

where M is an even number and "min" means that the number of summed terms takes the lower of i and $M/2$. The latter has the following form:

$$\mathfrak{f}(z)\cong\frac{\exp(\sigma z)}{Z}\times\left[\frac{1}{2}\mathfrak{f}(\sigma)+Re\sum_{k=1}^{K}\mathfrak{F}\left(\sigma+\frac{ik\pi}{z}\right)\exp\left(\frac{ik\pi}{Z}z\right)\right] \tag{25a}$$

where z corresponds to any point in the interval $0\le z<2Z$. In the application, a constant value of σZ can be chosen in the extent that $4<\sigma Z<5$, so that the truncation error can be recognized as sufficiently small. Assuming $z=Z$, one has:

$$\mathfrak{f}(Z)\cong\frac{\exp(\sigma Z)}{Z}\left[\frac{1}{2}\mathfrak{f}(\sigma)+\mathrm{Re}\sum_{k=1}^{K}\mathfrak{F}\left(\sigma+\frac{ik\pi}{Z}\right)(-1)^k\right] \tag{25b}$$

Both numerical algorithms have been successfully applied for predicting the transient behavior of heat exchangers in the previous work (Roetzel and Xuan, 1992). It should be pointed out that the first algorithm takes very little computation time and is suitable for calculating transient responses to most temperature variations without rapid oscillatory components; the second is fit to predict the response to oscillatory inlet disturbances but consumes more time because of the poor convergence of Fourier series, compared with the first. Therefore, one can select one of these algorithms to calculate the transient temperature profiles in the real time-domain from the transformed solutions in Eqs. 22, 23, 11 and 12 subject to the given inlet disturbances.

Theoretical Examples

Following the previously-outlined procedure, one can determine the transient performance of heat exchangers subject to arbitrary temperature variations and step flow disturbances, with consideration of the effect of flow maldistribution, heat capacities of both fluids, tube bank and the shell. These disturbances may occur at inlets separately or simultaneously and appear on either the shell and tube sides or simultaneously on both sides. Under the conditions that $U_{1r}=U_{2r}$, $R_\tau=1.0$, $Pe_r=Pe$, $n_1=0.6$ and $n_2=0.8$, some examples are calculated. Figure 2 illustrates the exit responses to step change in velocities on both sides with counterflow arrangement, and Figure 3 shows the responses to the linear temperature variations and step flow disturbances which take place simultaneously on both sides of a parallel flow heat exchanger.

In these figures, the initial states correspond to the previous steady state which exactly satisfies the energy balance, that is, $t_{2e}=R_{1r}(1-t_{1e})$ at $z=0$. Figure 2 shows that a transient process quickly approaches a new steady state under the given conditions. The energy balance between both fluids is also satisfied at this new steady state, which numerically demonstrates the feasibility that one can use the presented method to predict the transient performance of heat exchangers. As an example, Figure 3 shows the superposition of influences of temperature variations and step flow disturbances on the dynamic responses of an apparatus; under the conditions used in the calculation the influence of temperature changes is evidently dominant and the effect of flow disturbances increases with the values of U_{1r} (or U_{2r}).

Experimental Results

Transient experiments were carried out on a labor-sized heat exchanger with baffles to estimate the feasibility of the aforederived method. The working fluids were water. The shellside flow rate was suddenly altered by adjusting the rotational speed of the pump motor after the previous steady state had been reached. During the experiment, the shell and tubeside inlet

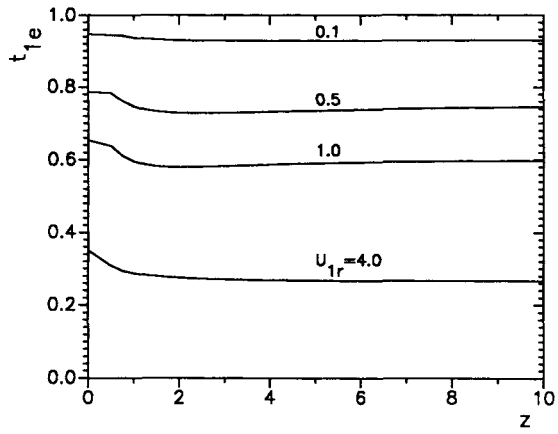

(a) shellside fluid

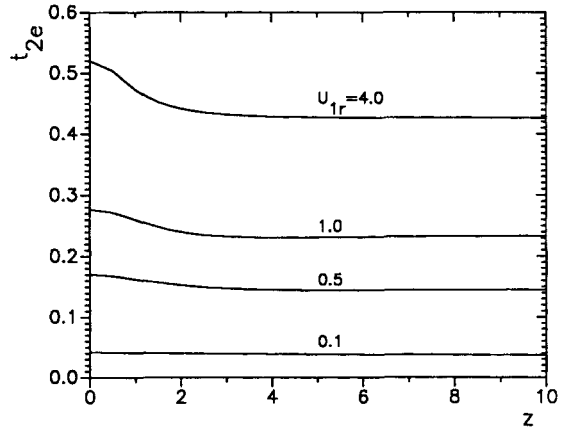

(b) tubeside fluid

Figure 2. Responses of exit temperatures t_1 and t_2 to step flow changes on both sides with counterflow arrangement ($R_{1r}=0.8$, $R_w=0.5$, $R_s=0.2$, $U_s/U_1=0.15$, $Pe=4.0$, $f_1(z)=1$, $f_2(z)=0$, $\sigma_1=0.8$ and $\sigma_2=1.1$).

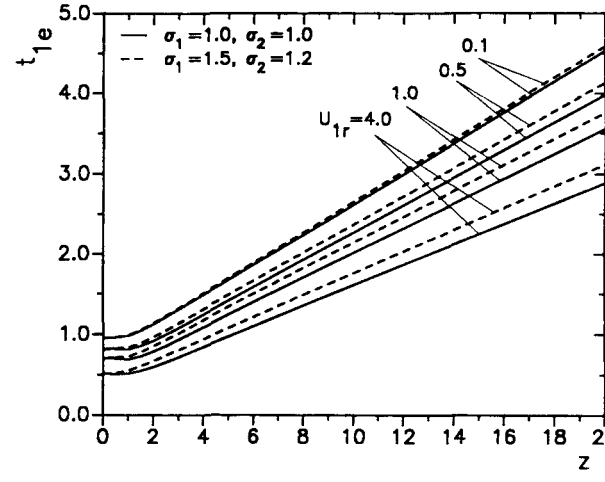

(a) shellside fluid

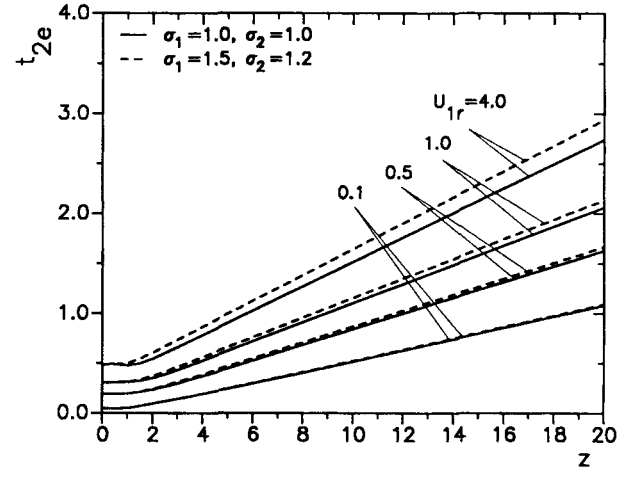

(b) tubeside fluid

Figure 3. Responses of exit temperatures t_1 and t_2 to linear temperature variations and step flow changes on both sides with parallel flow arrangement ($R_{1r}=1.0$, $R_w=0.4$, $R_s=0.3$, $U_s/U_1=0.2$, $Pe=6.0$, $f_1(z)=1+0.2z$, $f_2(z)=0.05z$, $\sigma_1=1.5$ and $\sigma_2=1.2$).

temperatures were allowed to be changeable. The clearance between the shell and the tube bank was changed by polyamid rings which have different thickness and could be embedded on the outside edges of baffles to examine the influence of maldistribution (leakage stream) on the transient behavior of the apparatus. The experiments were performed for the clearances $\delta=0.25$ and 2.45 mm with the parallel and counterflow arrangement. All inlet as well as exit temperatures and the flow rates were measured by thermoelements and turbine flowmeters, respectively. The readings were recorded and stored by a IBM-AT computer and a HP 3852A system which consists of a HP 44708A relay multiplexer with thermocouple compensation and a HP 44701A digital integrating voltmeter.

According to the measured inlet temperature changes and flow disturbances, the exit temperatures are calculated with the numerical inversion of Eqs. 22 and 23. For this purpose, the heat-transfer correlations on both sides and the values of the Péclet number Pe obtained from the previous steady-state experiments (Xuan, 1991) are used here. The comparison between the measured and calculated exit temperature profiles are plotted in the following figures. As the auxiliary information, the relevant inlet temperature profiles on both sides are also illustrated.

Figure 4 shows the exit temperature responses to an abrupt change of the shellside flow rate, that is, the shellside Reynolds number decreased from $Re_{1r}=7{,}700$ to $Re_1=2{,}770$ with a relatively constant tubeside Reynolds number $Re_2=3{,}477$ and the counterflow arrangement. The clearance between shell and tube bank is $\delta=0.25$ mm, in which the leakage stream is very small and this kind of maldistribution has little effect ($Pe=42$). In this case, the influence of heat capacity is negligible, and it is accurate enough to set $C_s=0$ or $U_s=0$. Figures 5 and 6 are pertinent to the clearance $\delta=2.45$ mm. Figure 5 corre-

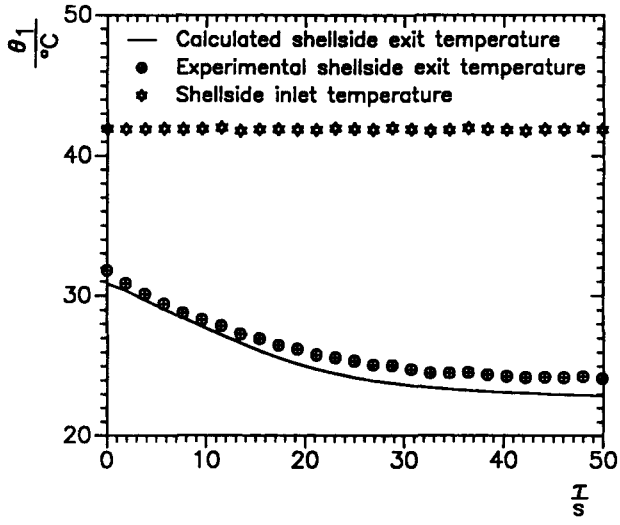

(a) shellside fluid

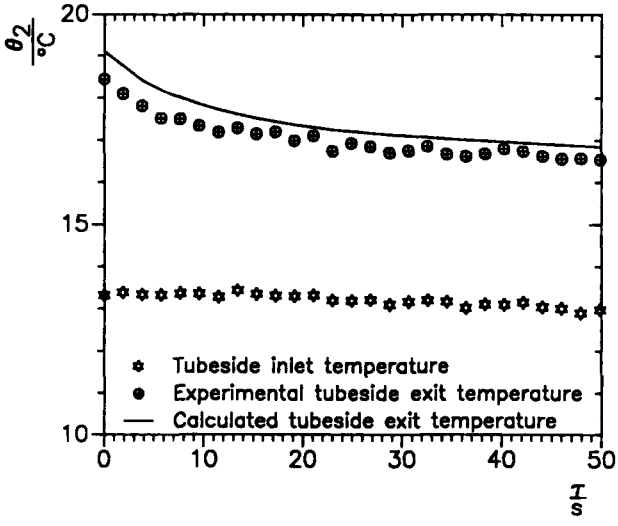

(b) tubeside fluid

Figure 4. Responses of exit temperatures t_1 and t_2 to a sudden decrease of shellside flow (counterflow and $\delta = 0.25$ mm).

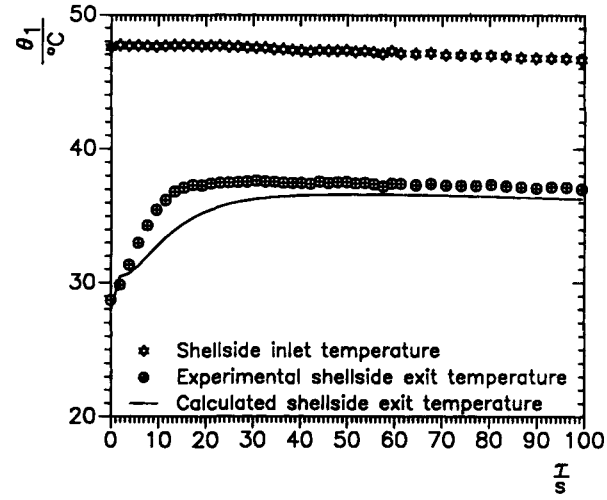

(a) shellside fluid

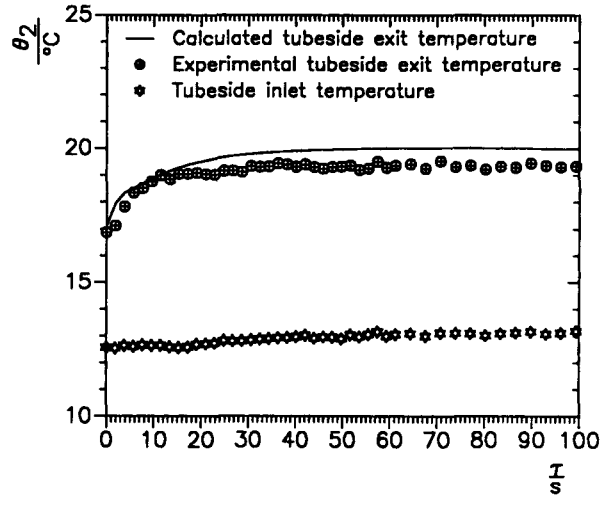

(b) tubeside fluid

Figure 5. Responses of exit temperatures t_1 and t_2 to an abrupt increase of shellside flow (counterflow and $\delta = 2.45$ mm).

sponds to the counterflow arrangement, a sudden increase of shellside flow rate with the Reynolds number from $Re_{1r} = 3{,}213$ to $Re_1 = 9{,}774$ and a constant $Re_2 = 3{,}213$ and Figure 6 to the parallel flow arrangement, a shellside flow step change from $Re_{1r} = 9{,}535$ to $Re_1 = 1{,}573$ and a constant $Re_2 = 3{,}170$. Because of the wider gap, the leakage stream was increased and the intensity of maldistribution became stronger. If this effect were neglected and a greater value of the Péclet number were inserted, there would be a greater deviation between the calculated and measured temperatures. In addition, the effect of heat capacity of the shell was noticeable, especially in the strongly transient phase ($\tau < 20$). For the calculation of exit temperature profiles illustrated in these two figures, $U_s = U_1$ was assumed. The comparison has shown that there is a satisfactory agreement between the calculated and experimental results, which demonstrates that the previously derived method is feasible to predict the transient behavior of heat exchangers. Furthermore, a quite good reproduction of such an agreement appeared for different runs at the same Reynolds numbers, clearance and flow arrangement which have been not shown here because of the limited space.

These figures show that the shell and tubeside inlet temperatures did not remain constant and were also changed during the experiment, although the main object of the experiment was to discuss the transient response to a step change of flow rate. But it causes no difficulties for the theoretical prediction since the method includes both temperature variations and flow disturbances. It is essential to consider the effect of the shell if one wants to make reasonable predictions, especially for a short time after the instant of a transient process. This effect

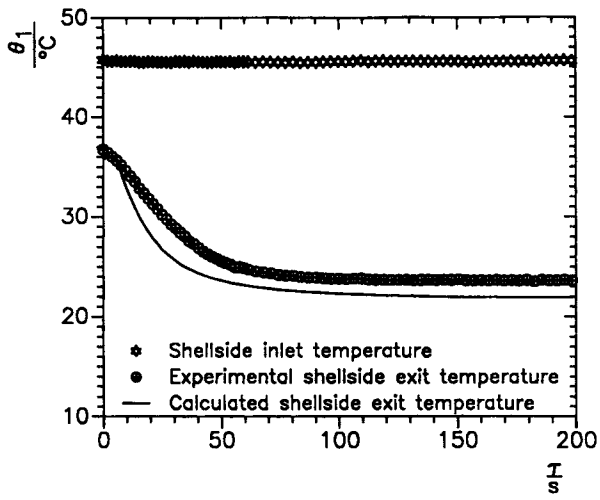

(a) shellside fluid

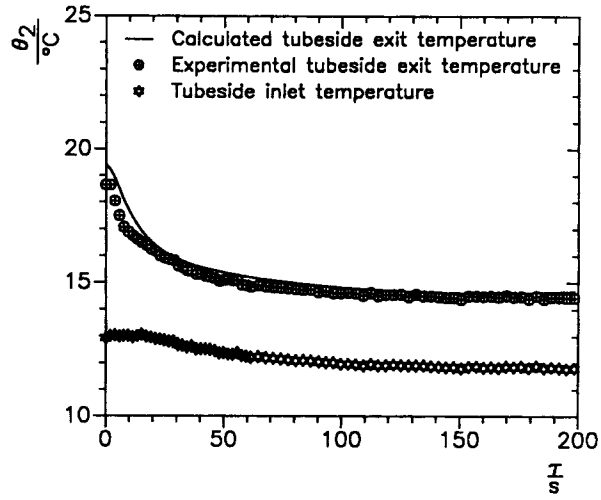

(b) tubeside fluid

Figure 6. Responses of exit temperatures t_1 and t_2 to a sudden decrease of tubeside flow (parallel flow and $\delta = 2.45$ mm).

depends not only upon the value of the heat capacity of the shell but also upon the heat exchange between the shell and the shellside fluid. If the clearance between shell and tube bank is small, the influence of the shell is negligible; otherwise one must set up an equation for the temperature profile of the shell in the model.

Introducing the parameter *Pe* into the model, one has the possibility to quantitatively describe the influence of maldistribution. The Péclet number *Pe* depends upon the intensity of maldistribution and should be determined by experiment at present for the complicated flow pattern in shell-and-tube heat exchangers with baffles. In this article its value obtained in the previous work has been used. If necessary, the proposed model can also be applied to the plug flow by simply setting $Pe \to \infty$. Both dispersion and plug-flow models give almost the same results if $Pe > 60$. It is expected that the effect of flow maldistribution becomes stronger for a high value of NTU and laminar flow. In other words, the application of the dispersion model will be of greater importance for high values of NTU and low values of *Pe*.

Conclusions

The transient performance of heat exchangers subject to arbitrary temperature and step flow disturbances has been investigated. A simple, versatile, and efficient method based on the dispersion model has been derived, including heat capacities of both fluids, tube bank and shell. Such temperature and flow variations are allowed to occur on either side or both sides and separately or simultaneously. Two types of numerical inversion algorithms have been used and discussed. The Gaver-Stehfest algorithm may be the first choice, because it costs little time; but the Fourier series technique is more powerful to calculate the response to disturbances with oscillatory components. The examples of numerical calculation have proven the satisfactory accuracy of the proposed method.

The transient experiment has been executed on a labor-sized heat exchanger with baffles. The good agreement between the calculated and measured temperature profiles has verified the feasibility of the theoretical method. The effect of the shell should be considered to correctly predict the transient response. The influence of maldistribution on the transient process can be explained by the Péclet number *Pe*.

Acknowledgment

The authors would like to express their thanks to the Deutsche Forschungsgemeinschaft for the financial support of this research work.

Notation

A = heat-transfer area, m^2
A_q = transverse flow area of shellside fluid, m^2
C = heat capacity, J/K
$\mathfrak{D}$ = dispersion coefficient or apparent heat conductivity, W/m·K
$f_1(z), f_2(z)$ = inlet temperature changes
$F_1(z), F_2(s)$ = transformed forms of $f_1(z)$ and $f_2(z)$ in the Laplace image domain
h = heat-transfer coefficient, W/m^2·K
L = length of the heat exchanger, m
ℓ = distance from the entrance of shellside fluid, m
Pe = Péclet number
Re = Reynolds number
s = variable of the Laplace transform
t = dimensionless temperature, $t = (\theta - \theta_{2r})/(\theta_{1r} - \theta_{2r})$
T = transformed form of t in the Laplace image domain
u = velocity of fluid, m/s
$\dot{W}$ = thermal flow rate, W/K
x = dimensionless distance, $x = \ell/L$
z = dimensionless time, $z = \tau/\tau_{r1}$

Greek letters

δ = clearance between shell and tube bank, mm
θ = temperature, K (°C)
θ_{1r}, θ_{2r} = two different reference temperatures, K (°C)
τ = time, s
τ_r = residence time of fluid in the heat exchanger, s

Subscripts

1, 2 = shell and tube sides, respectively
e = exit
r = previous steady state
s, w = shell and tube bank, respectively

Literature Cited

Boyce, W. E., and R. C. DiPrima, *Elementary Differential Equations and Boundary Value Problems*, 3rd ed., Wiley, New York (1977).

Correa, D. J., and J. L. Marchetti, "Dynamic Simulation of Shell-and-Tube Heat Exchangers," *Heat Transf. Eng.*, **8**(1), 50 (1987).

Incropera, F. P., and D. P. Dewitt, *Fundamentals of Heat and Mass Transfer*, Wiley, New York (1985).

Ratel, G., P. Mercier, and G. Icart, "Heat Transfer in Transient Conditions," *Design and Operation of Heat Exchangers, Proceedings of the Eurotherm Seminar No. 18*, W. Roetzel, P. J. Heggs, and D. Butterworth, eds., Hamburg, Germany, Springer-Verlag, Berlin, p. 111 (1992).

Roetzel, W., and Y. Xuan, "Transient Response of Parallel and Counterflow Heat Exchangers," *J. Heat Transf.*, **114**, 510 (1992a).

Roetzel, W., and Y. Xuan, "Analysis of Transient Behaviour of Multipass Shell and Tube Heat Exchangers with the Dispersion Model," *Int. J. Heat Mass Transf.*, **35**, 2953 (1992b).

Roetzel, W., and Y. Xuan, "Prediction of Dynamics of Parallel and Counterflow Heat Exchangers with the Dispersion Model," submitted to *J. Heat Transf.* (1992c).

Romie, F. E., "Transient Response of the Counterflow Heat Exchanger," *J. Heat Transf.*, **106**, 620 (1984).

Romie, F. E., "Transient Response of the Parallel-Flow Heat Exchanger," *J. Heat Transf.*, **107**, 727 (1985).

Satoshi, I., and A. Kishima, "Application of Fourier Series Techniques to Inverse Laplace Transform," *Kyoto Univ. Memories*, **34**, part I, 53 (1972).

Stehfest, H., "Numerical Inversion of Laplace Transform," *Communication of the ACM*, **13**, 47 (1970).

Tan, K. S., and I. H. Spinner, "Dynamics of a Shell-and-Tube Heat Exchanger with Finite Tube-Wall Heat Capacity and Finite Shell-Side Resistance," *Ind. Eng. Chem. Fundam.*, **17**(4), 353 (1978).

Tan, K. S., and I. H. Spinner, "Numerical Methods of Solution for Continuous Countercurrent Processes in the Nonsteady State," *AIChE J.*, **30**, 770 (1984).

Tinker, T., "Shell Side Characteristics of Segmentally Baffled Shell-and-Tube Heat Exchangers, Parts I, II and III," *Proc. General Discussion on Heat Transfer*, IMechE, London, p. 89 (1951).

Xuan, Y., *Thermische Modellierung mehrgängier Rohrbündelwärmeübertrager mit Umlenkblechen und geteiltem Mantelstrom*, Fortschr.-Ber. VDI Reihe 19 Nr. 52. VDI-Verlag, Düsseldorf (1991).

Yang, W. J., "Transient Heat Transfer in a Vapor-Heated Heat Exchanger with Arbitrary Timewise-Variant Flow Perturbations," *J. Heat Transf.*, **86**, 133 (1964).

Zukauskas, A., and R. Ulinskas, *Heat Transfer in Tube Banks in Crossflow*, Hemisphere Publishing, New York (1988).

Manuscript received Mar. 10, 1992, and revision received July 30, 1992.